THE ASTROPHYSICAL JOURNAL, 454:L1–L6, 1995 November 20


# PERFORMANCE AND PRELIMINARY CALIBRATION OF THE HOPKINS ULTRAVIOLET TELESCOPE ON THE ASTRO-2 MISSION

JEFFREY W. KRUK, SAMUEL T. DURRANCE, GERARD A. KRISS, ARTHUR F. DAVIDSEN, WILLIAM P. BLAIR, AND BRIAN R. ESPEY
Department of Physics and Astronomy, Johns Hopkins University, Baltimore, MD 21218

AND

DAVID S. FINLEY
Eureka Scientific, Berkeley, CA 94602
*Received 1995 July 5; accepted 1995 September 7*

## ABSTRACT

An improved version of the Hopkins Ultraviolet Telescope (HUT) made its second flight on the Astro-2 mission aboard the Space Shuttle *Endeavour* from 1995 March 2–18. The longer mission duration and greatly improved pointing stability relative to Astro-1 made possible 385 observations of 265 celestial targets at far-ultraviolet wavelengths. Observing efficiency exceeding 60% over 14 days of science operations yielded 205 hr of on-source integration time, a factor of 5.1 increase over Astro-1.

We describe changes to the instrument following Astro-1 and the in-flight photometric calibration, which is based on a comparison of our observations of the hot DA white dwarf HZ 43 with a model atmosphere whose parameters were derived from optical observations. The peak effective area is 24.1 $cm^2$ at 1160 Å, where the inverse sensitivity is $7.09 \times 10^{-13}$ ergs $cm^{-2}$ $count^{-1}$. This is an improvement by a factor of 2.3 over Astro-1, largely attributable the installation of new optics coated with ion-sputtered silicon carbide. Observations of several other white dwarfs indicate that the calibration is accurate to about 5%, after correction for modest, but significant, time-dependent degradation during the mission. The spectral resolution varied from 2 to 4 Å over the first-order wavelength range of 820–1840 Å. The wavelength scale is established to better than 1 Å. As on Astro-1, dark counts and scattered light were extremely low. Airglow line intensities were much lower because of the lower level of solar activity. When all factors are considered together, HUT performance on Astro-2 was a full order of magnitude better than that achieved on the highly successful Astro-1 mission.

*Subject headings:* instrumentation: detectors — instrumentation: spectrographs — space vehicles — telescopes — ultraviolet: general

## 1. INTRODUCTION

The first flight of the Hopkins Ultraviolet Telescope (HUT) aboard the Astro-1 space shuttle mission in 1990 December clearly demonstrated the value of far-UV spectrophotometry for many diverse areas of astrophysical research (Davidsen 1993). HUT is designed to observe faint sources at moderate resolution (3 Å) in the (first-order) wavelength range 820–1840 Å. It thus overlaps with the spectroscopic capabilities of the *Hubble Space Telescope* (*HST*) at $\lambda > 1200$ Å and provides an important complementary capability for studies of the little-explored, but astrophysically interesting, 912–1200 Å region. By employing just two reflections, special optical coatings, and a windowless detector system, HUT achieves a sensitivity equal to that of the Faint Object Spectrograph (FOS) on *HST* at about 1200 Å (Keyes et al. 1995) and maintains high sensitivity down to the Lyman limit (Davidsen et al. 1992).

Prior to the flight of Astro-1, spectroscopic studies at far-UV wavelengths were essentially limited to high-resolution work on very bright stars with *Copernicus* (Rogerson et al. 1973) and very low resolution observations with *Voyager* (Holberg 1991). More recently, there has been some further work at these wavelengths with *ORFEUS* (Grewing et al. 1991; Hurwitz & Bowyer 1991). HUT carried out the first extensive moderate resolution work at wavelengths from Ly$\alpha$ to the Lyman limit.

The success of HUT on Astro-1 was tempered somewhat by the relatively short mission duration (9 days) and by difficulties encountered with the Spacelab Instrument Pointing System (IPS). NASA's decision to refly HUT on the Astro-2 mission provided the opportunity to correct these deficiencies and also to make significant improvements in HUT's performance, which are described here. A factor of 2.3 increase in sensitivity was achieved, primarily through replacing the primary mirror and diffraction grating with new ones coated with previously unavailable, ion-sputtered silicon carbide. IPS hardware and software problems were corrected, resulting in excellent pointing performance, with 1″ stability obtained routinely. An extended-duration mission totaling 16 days, the longest space shuttle flight conducted to date, enabled us to capitalize fully on these improvements.

A guest investigator program for Astro-2 expanded the scope of scientific topics addressed with HUT. Altogether, about 20 scientific programs were successfully conducted. We obtained 385 observations of 265 different celestial targets, with a total on-source integration time of 205 hr. The excellent performance of HUT/Astro-2 was highlighted by our success in observing the quasar HS 1700+64 ($V = 16.1$, $z = 2.74$, $F_\lambda(1000\ \text{Å}) \sim 5 \times 10^{-16}$ ergs $cm^{-2}$ $s^{-1}$ $Å^{-1}$), toward which the opacity of singly ionized intergalactic helium was measured (Davidsen, Kriss, & Zheng 1995). In this Letter we describe the changes made to HUT and its performance on Astro-2, including a preliminary but detailed calibration.

## 2. INSTRUMENTATION

Davidsen et al. (1992) provide a full description of HUT, including its performance, as flown on the Astro-1 mission in 1990 December. Following Astro-1, the original 0.9 m, f/2 iridium-coated Zerodur primary mirror was replaced with the nearly identical Cervit backup mirror, which had been overcoated with silicon carbide (SiC) by the Optical Thin Film Laboratory at Goddard Space Flight Center. SiC has a reflectivity of 30%–40% over the first-order wavelength range of 820–1840 Å, nearly twice that of the original iridium coating, but in second order it is much lower, dropping to less than 10% below 600 Å (Keski-Kuha et al. 1988; McCandliss et al. 1994). To retain good optical reflectivity for the acquisition TV camera, the SiC was deposited directly over the original iridium, and its thickness (1400 Å) was tailored accordingly. The resulting approximately 57% optical reflectivity is comparable to the 65% of the original iridium coating. Iridium was chosen originally for its high reflectivity combined with good stability in a space environment. SiC is susceptible to damage by high-velocity atomic oxygen (Herzig, Toft, & Fleetwood 1993) but is otherwise stable. To protect the mirror surface, we avoided pointing the telescope within 20° of the shuttle velocity vector whenever the doors were open.

The near–normal-incidence Rowland-circle spectrograph employed the same optical and mechanical design as that flown on Astro-1, except that the holographically ruled, 20 cm diameter f/2 grating was coated with SiC instead of osmium. The selection of apertures provided by the eight-position rotating mechanism at the spectrograph entrance was revised for Astro-2 to reflect the chosen scientific programs. Two positions for ground operations (a vacuum seal position and a large aperture for calibration) were retained. There were three circular apertures of 12″, 20″, and 32″ diameter, and two long-slit apertures with dimensions of $10'' \times 56''$ and $19'' \times 197''$. The long slits provide spectral resolutions of 3.5 and 7 Å, respectively, for diffuse sources. The remaining position, unused during Astro-2, contains a thin aluminum filter behind a 32″ diameter aperture, which provides a pure extreme-ultraviolet (EUV) bandpass (415–800 Å). The apertures were etched into a mirrored surface that reflects visible light from the surrounding star field to the TV acquisition camera. For Astro-2 the mirrored surface was polished to a higher quality optical finish to improve the throughput of the TV acquisition system.

The design of the Astro-2 HUT detector differed from that flown on Astro-1 only in the microchannel plate (MCP) mounting washers and the electron repeller grid mounted just in front of the photocathode surface of the MCPs. The new mounting washers were dimpled to provide increased conductance for pumping the region between the MCPs and the phosphor anode, and they were gold plated to minimize the potential for vibration-induced problems with electrical contact. The new electron repeller grid consisted solely of two wires strung parallel to the dispersion direction and located just outside the light path for the small aperture door states. The CsI photocathode was deposited on the MCPs in 1993 June. Monitoring of the count rate produced by the 1849 Å line of a mercury calibration lamp imaged onto the detector by the grating throughout the preflight integration process showed a slow degradation in the photocathode response over time similar to that observed prior to Astro-1.

The HUT detector is limited to total count rates less than 5000 counts $s^{-1}$. To observe brighter targets, principally the brightest O and B stars, the HUT telescope aperture may be reduced from the nominal full aperture size of 5120 $cm^2$. A 50% reduction is accomplished by closing one of two semicircular shutter doors. Further reduction to 1% (50 $cm^2$) and 0.02% (1 $cm^2$) of full aperture can be made by closing both shutter doors and opening either of two small apertures. The 1 $cm^2$ aperture was not used during the Astro-2 mission. Software changes to the on-board Dedicated Experiment Processor (DEP) for Astro-2 permitted the large shutter doors to be partially opened to specified, reproducible, aperture areas. Two such partial openings, which exposed 200 $cm^2$ or 750 $cm^2$ of the primary mirror, were used routinely during Astro-2.

## 3. PERFORMANCE

The Astro-2 mission began at UT 06:38:13 on 1995 March 2 with the launch of the space shuttle *Endeavour* (STS-67). The orbit was nearly circular at an altitude of 352 km and an inclination of 28°.5. Instrument activation started at 00:03:44 (days:minutes:hr) Mission Elapsed Time (MET), and first light occurred at 00:20:56 MET with an observation of Capella. Science operations began at 01:02:45 MET and continued with only minor interruptions until the instruments were deactivated at 14:23:35 MET. Observing efficiency was low during the first day of science operations while the target acquisition and tracking procedures were refined, but it was in accordance with premission expectations thereafter. Pointing stability was frequently as good as 1″ rms, though the absolute pointing error could be several arcseconds. The performance of HUT itself was nominal in nearly all respects throughout the flight, with two significant exceptions: a discrepancy between the best focus for the camera and spectrograph, and a gradual decrease in the instrument throughput during the flight, which are discussed in detail below.

### 3.1. *Alignment and Focus*

Observations made during the activation period were used to determine the primary mirror position giving the best focus for both the spectrograph and acquisition camera. The camera optics had been adjusted during instrument assembly to make these two mirror positions coincide, but on-orbit they were found to differ by 200 $\mu$m. The cause of this change is not understood; it is presumably due to the shifting of some component during launch. For most observations the mirror was set halfway between these two positions, which gave camera images of about 4″.5 FWHM. For some observations with faint guide stars, however, the mirror was set at the position giving the best camera focus (about 3″.3 FWHM). The spectrograph line-spread function is determined primarily by the fact that the flat detector surface does not coincide with the curved Rowland circle. Changing the focus position of the primary mirror shifts the point at which these two surfaces intersect. The compromise mirror position resulted in minima in the line-spread function at 900 and 1600 Å, instead of the intended locations of 1050 Å and 1350 Å.

Measurements of the in-flight point-source spectral resolution utilized unresolved emission lines in stellar spectra. The initial determination of spectral resolution as a function of mirror position was done with the early observation of Capella; more detailed measurements were subsequently made with spectra of the symbiotic stars RR Tel, AG Dra, V1016 Cyg, and Z And, obtained as part of the Guest

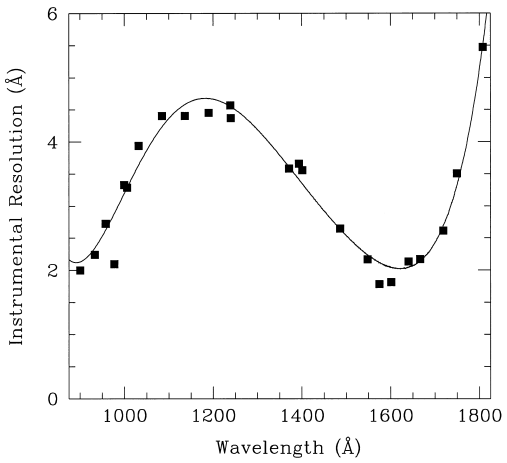


FIG. 1.—The resolution of HUT for the Astro-2 mission is shown as a smooth curve. Points (*squares*) are measured from unresolved emission lines in the spectrum of the symbiotic star RR Tel.

Investigator program of B. Espey. The spectrum of RR Tel provided the bulk of the line measurements because of its high signal-to-noise ratio and the presence of lines across the entire HUT bandpass (Espey et al. 1995). Since Gaussians were found to provide a good fit to single emission lines, Gaussian deblending using the SPECFIT software (Kriss 1994) was used to obtain the location and line width of blended features. The relative strength of lines observed in *IUE* high-resolution spectra were used where necessary to help in the deblending process. The resulting resolution, illustrated in Figure 1, was found to be 2 Å FWHM at 900 Å and 1600 Å with a broad maximum of about 4 Å FWHM over 1100–1250 Å.

### 3.2. *Wavelength Scale*

The wavelength scale was determined using known positions of narrow emission lines in the symbiotic star spectra listed above. Aside from small offsets necessary to correct for telescope pointing errors along the dispersion direction, the results for different objects proved consistent within measurement error. These measurements revealed deviations from a linear wavelength scale by as much as 1.5 Å. The data were fitted with a four-term Legendre polynomial, resulting in an rms error of 0.236 Å. Additional terms did not significantly reduce the overall rms error of the fit. Comparison of laboratory and in-flight positions of Ly$\alpha$, Ly$\beta$, and the calibration lamp lines shows agreement to within 1 pixel (0.51 Å), indicating no disturbance of the internal spectrograph alignment during launch.

Consistency checks of the wavelength scale were made using measurements of spectra in which the slit was uniformly illuminated and which therefore do not require telescope pointing corrections to the wavelength scale. The extended sources chosen for this purpose were a daytime airglow spectrum and a lunar (essentially solar) spectrum. Although the rms deviations about the adopted wavelength scale are larger because of the increased line width and blending, the data indicate that the mean offset of the wavelength scale is less than 0.2 Å.

### 3.3. *Instrument Sensitivity*

The instrument sensitivity for full-aperture observations was determined by comparing observations of the hot DA white dwarf HZ 43 with the model atmosphere for this star calculated by one of us (D. S. F.), using D. Koester's model atmosphere codes (Koester, Schulz, & Weidemann 1979; Finley, Koester, & Basri 1995). The parameters for this model are $T_{\rm eff}$ = 49,000 K, $\log g$ = 8.0, and $V$ = 12.91. $T_{\rm eff}$ and $\log g$ were determined from fits to Balmer line profiles (Finley et al. 1995), while the $V$ magnitude was measured by the FOS (Bohlin, Colina, & Finley 1995). The models incorporate the Hummer-Mihalas occupation probability formalism (Hummer & Mihalas 1988) with the critical field strength parameter set to twice the nominal value (Bergeron 1993). The model was corrected for transmission through the interstellar medium, assuming a hydrogen column density of $\log N_{\rm H\,I} = 17.83$ and $b$ = 10 km s$^{-1}$. Extinction by dust was assumed to be negligible. The resulting model flux was then convolved with a Gaussian of 3 Å FWHM to simulate the instrumental resolution.

HZ 43 was observed three times during the mission (at 35, 64, and 329 hr MET). The last pointing contained the longest periods of clean photometric data and was therefore used to define the effective area. Following acquisition, a 470 s integration was obtained through the 20″ round slit, followed by a 696 s integration through the 32″ round slit; both integrations were entirely within orbital night. The observed count rates were the same for the two integrations, and the count rate fluctuations on a 2 s timescale are consistent with Poisson noise, indicating that both portions of the observation are photometric. We therefore combined the two spectra and applied the following corrections. (1) Pulse pile-up: this is event loss caused by the arrival of overlapping events on the photodiode array within the 1 ms readout time; this effect and the correction scheme are described in Kruk et al. (1995). The peak correction is 9% at 1085 Å, dropping to $\leq$1% at either end of the spectrum. (2) Dark count subtraction: 0.01%–0.1%; see § 3.5. (3) Scattered light subtraction: 0.005%–0.1%; see also § 3.5. (4) Second-order subtraction: the equivalent of 21% of the counts Å$^{-1}$ in the 912–920 Å region contribute in second order at 1824–1840 Å. This excess is subtracted from the data. The EUV flux (less than 912 Å) appearing in second order is estimated to peak at about 1% of the counts at 1550 Å, drop to 0.5% at 1300 Å and 1650 Å, and drop rapidly to zero shortward of Ly$\alpha$. This EUV flux was ignored in the present calibration but will be included in future revisions. (5) Flat-field corrections: see § 3.4. (6) Time dependence of the instrument throughput: see below.

To produce the instrument sensitivity curve, we divided the corrected count spectrum into the model flux spectrum. Dividing this into the energy per photon as a function of wavelength and dividing by the (slightly variable) pixel width gives the effective area, which is shown in Figure 2. The peak effective area is 24.1 cm$^2$ at 1160 Å, where the corresponding inverse sensitivity is $7.09 \times 10^{-13}$ erg cm$^{-2}$ count$^{-1}$. For comparison, we also show the final effective area curve for the Astro-1 version of HUT (Kruk et al. 1995). As was the case on Astro-1, the effective area measured in-flight is in fairly good agreement with the preflight laboratory calibration shortward of about 1050 Å but falls roughly 30% below it at longer wavelengths. This difference is believed to be due to aging of the CsI photocathode.

The stability of the instrument throughput was monitored by making multiple observations of the DA white dwarf GD 394 (at 64, 92, 138, 211, and 341 hr MET), in addition to the three observations of HZ 43 listed above. The sensitivity was found

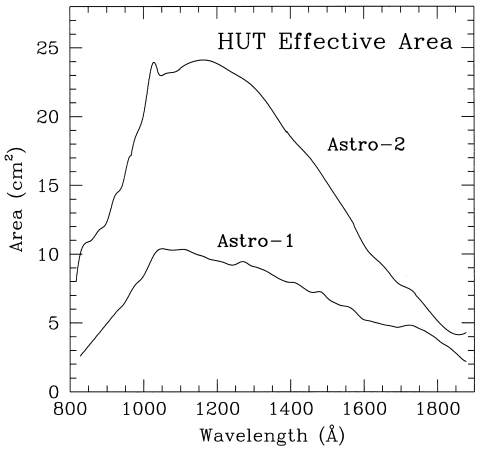


FIG. 2.—The first-order effective areas of HUT for both Astro-1 and Astro-2 are shown. The Astro-2 curve is the effective area at the start of the mission; corrections for time dependence are described in the text.

to decline gradually over the course of the mission in a wavelength-dependent fashion. The total decline was relatively small at long wavelengths (5% at 1800 Å) and rose steadily toward shorter wavelengths (27% at 912 Å). The rate of decline was greatest early in the mission, with roughly one-half of the total decline occurring prior to 100 hr MET and 75% of the total decline occurring by 138 hr MET. A family of correction curves was calculated by fitting three-term Chebyshev polynomials to the ratios of late-to-early observations of HZ 43 and GD 394. These correction factors are shown in Figure 3. A correction curve for any given MET can be obtained by interpolating among the curves.

Neither the wavelength dependence nor the time dependence of this degradation matches that of the detector exposure: the total flux per unit area on the detector has a broad maximum over 1100–1350 Å and drops rapidly toward either end of the detector, and it increases with time during the mission primarily during observations of a relatively small number of bright stars. Both, however, are consistent with possible degradation of the primary mirror. Two possible mechanisms for this are condensation of contaminants onto the mirror, and oxidation of the SiC coating by energetic atomic oxygen. One of the witness mirrors removed from the

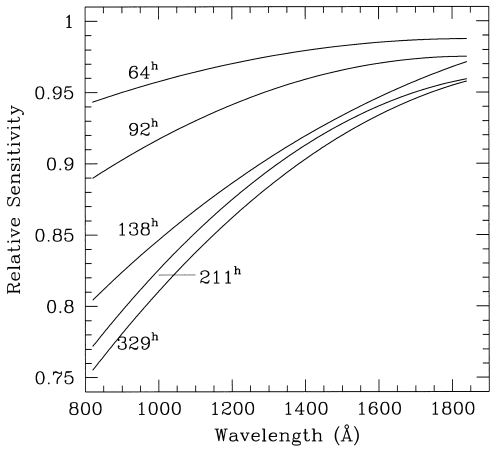


FIG. 3.—The family of curves labeled in MET shows the time dependence of the loss in sensitivity of HUT as a function of wavelength throughout the Astro-2 mission. The cause of the degradation is still under investigation.

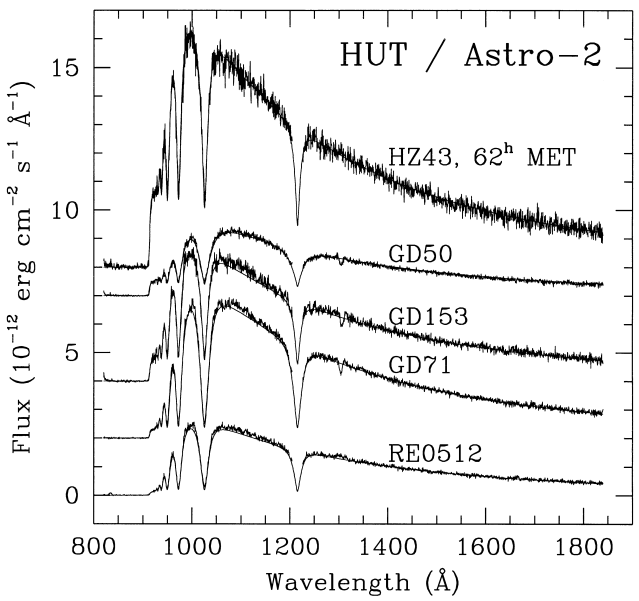


FIG. 4.—Observed spectra of five white dwarfs observed during Astro-2, flux-calibrated with the effective area curve derived from the observation of HZ 43 at 329 hr MET, are compared to predicted fluxes from the model atmospheres convolved with the instrument resolution function. The largest deviations visible are in the 1000–1200 Å range; they are less than 5%. All five objects are plotted on the same absolute flux scale, with zero-level offsets that can be read from the figure.

telescope shortly after the flight shows similar degradation and is being investigated further.

An internal consistency check on the white dwarf models and on our data reduction procedures can be made by comparing the observed flux with the model predictions for other hot DA white dwarf stars spanning a range of effective temperatures and surface gravities. We observed GD 71, GD 153, RE 0512−004, GD 50, Wolf 1346, and RE 1738+669 through the full aperture as part of the Guest Investigator program of D. Finley, D. Koester, and R. Kimble. These spectra were reduced and compared with models in the same manner as described above for HZ 43. As shown in Figure 4, for GD 71, GD 153, RE 0512−004, and GD 50, the observed spectra agree with the models to better than 5%. The parameters for the models shown are as follows: GD 71, $T_{\rm eff}$ = 32,300 K, $\log g$ = 7.73, $V$ = 13.032; GD 153, $T_{\rm eff}$ = 38,500 K, $\log g$ = 7.67, $V$ = 13.353; RE 0512−004, $T_{\rm eff}$ = 32,000 K, $\log g$ = 7.4, $V$ = 13.80; and GD 50, $T_{\rm eff}$ = 41,000 K, $\log g$ = 9.2, $V$ = 14.00. All of the model parameters were derived from fits to Balmer line profiles and from $V$-band photometry (Finley et al. 1995). For Wolf 1346 the observed spectrum agrees with the model to within measurement errors, except for wavelengths 1080–1150 Å (between the broad merging absorption wings of Ly$\alpha$ and Ly$\beta$), where the data exceed the model by as much as 18%. The observed flux for RE 1738+669 is consistent with the *IUE* flux; comparisons with the model flux will require corrections for interstellar extinction and molecular hydrogen that are still in progress.

The instrument throughput for door configurations other than fully open was determined by taking ratios of spectra obtained through more than one door state on the same object. Since the various door states illuminate different regions of the mirror, grating, and detector (and illuminate the detector at different angles), the corresponding throughputs

differ by more than just the relative exposed areas of the mirror.

The throughput for the half-open door state was determined by obtaining spectra of both HZ 43 and GD 153 through both the full and half-open door states. The two sets of spectra gave essentially similar ratios of half to full door flux, so the two ratios were averaged. The resulting throughput ratio rises from 0.475 at 912 Å to 0.50 at 1400 Å and then declines gradually to 0.415 at 1830 Å.

The 750 $cm^2$ door state was calibrated by two different means: by observing GD 394 through this door as well as through the full aperture, and by direct observation of the hot DA white dwarf G191–B2B. The data for G191–B2B were reduced in the same manner as described above for HZ 43. The model atmosphere parameters used for G191–B2B were $T_{\rm eff}$ = 60,000 K, log $g$ = 7.4, and $V$ = 11.79. This model differs by $\lesssim$2% from that used to define the HUT calibration for Astro-1. In order to keep any model dependence in the calibration the same for all door states, however, the effective area curve for this door state was determined by fitting a two-piece cubic spline to the ratio of the G191–B2B–derived effective area and the HZ 43–derived full aperture effective area, and then multiplying by the full aperture effective area. This retains the large-scale wavelength dependence of the G191–B2B effective area determination but should remove any additional small-scale artifacts introduced by small errors in the model parameters, mismatches between the model and the actual spectral resolution, etc. The observations of GD 394 gave results that were consistent with the G191–B2B calibration, but with considerably poorer statistics.

The 200 $cm^2$ door state was also calibrated by an observation of G191–B2B. The data reduction procedures were the same as for the 750 $cm^2$ observation. The ratio of the two spectra was nearly independent of wavelength and was equal to 0.273, quite close to the nominal ratio of geometric areas (0.267).

The 50 $cm^2$ door state was calibrated by observing the hot sdO star BD +75°325 through both the 200 $cm^2$ and 50 $cm^2$ doors. Longward of 1025 Å the ratio of the two spectra is independent of wavelength and is equal to 0.273; shortward of 1025 Å the ratio drops smoothly to about 0.24 at 912 Å. The effective area for the 200 $cm^2$ door derived from the G191–B2B measurement was scaled by this ratio to determine the 50 $cm^2$ door effective area. Since the calibration for these two door states is the furthest removed from the HZ 43–derived full aperture calibration, a test of our data reduction and calibration procedures can be made by comparing our spectrum for BD +75°325 with that obtained by the FOS (kindly provided by R. Bohlin). The HUT and FOS spectra for this star are shown in Figure 5, for the wavelength region common to both instruments. The two spectra agree to within 5% at most wavelengths and to within 10% everywhere.

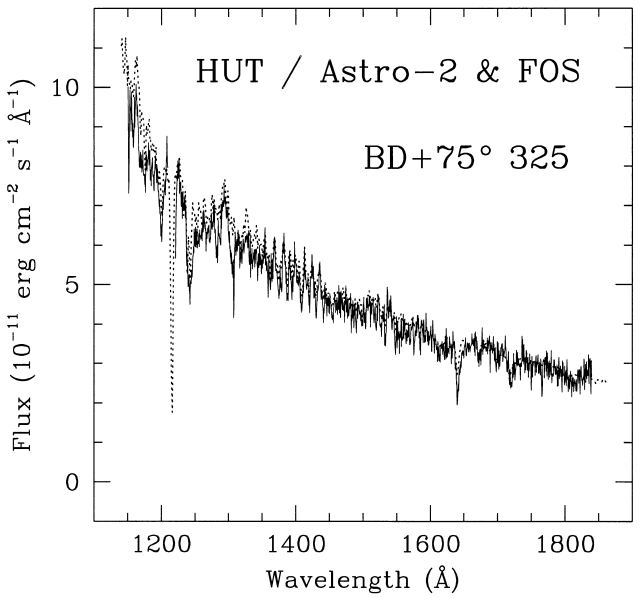


FIG. 5.—The HUT spectrum of BD +75°325 (*solid line*), compared to the FOS spectrum (*dotted line*). Apart from the few uncorrected flat-field features in the HUT spectrum (see text), the two spectra agree to within 10%; over most of the spectrum the differences are less than 5%.

### 3.4. *Detector Performance*

The gain of the detector had been monitored with the calibration lamp over the 18 month interval between spectrograph integration and launch. The gain declined steadily over this period, necessitating an increase in detector voltage at the start of the mission to restore the detector to its proper operating point. The detector gain was monitored frequently during the mission, which revealed a small decline over the first 160 hr. The detector high voltage was then raised slightly to maintain the pulse-height distribution at its nominal position, and the detector gain remained stable thereafter. This voltage increase resulted in an increase in the quantum detection efficiency (QDE) of roughly 3%.

Localized regions of the detector exhibited more significant gain decreases over the course of the mission, as expected, caused by "scrubbing" by bright emission lines. The intense geocoronal emission lines at Ly$\alpha$ and O I $\lambda$1304 Å resulted in almost complete loss of QDE at the centers of the lines. Much weaker localized depressions in detector QDE were found as well, arising from the O I $\lambda$989 Å airglow emission and the bright Wolf-Rayet star emission lines N V, C IV, and He II. These features are time and door-state dependent. By the end of the mission, these features had equivalent widths of 0.2–0.3 Å. Corrections for these features are not included in the present calibration but will be in future versions. Three similar gain-loss features are included in the present calibration, since they appear to have been induced by calibration lamps used in preflight instrument processing and do not appear to vary during the mission. These three features are at 1048, 1066, and 1664 Å, and have equivalent widths of 0.28, 0.20, and 1.34 Å, respectively.

### 3.5. *Backgrounds: Dark Counts, Airglow, and Scattered Light*

The dark count level was low, averaging $7.3 \times 10^{-4}$ counts $s^{-1}$ $Å^{-1}$ and $9.0 \times 10^{-4}$ counts $s^{-1}$ $Å^{-1}$, respectively, for the two detector voltages used during the mission. The dark count increased by as much as a factor of 30 during passages through the South Atlantic Anomaly (SAA) but remained too low to have a significant effect on observations of bright targets planned during these periods.

Because of its large apertures, HUT is particularly sensitive to airglow. Flying near solar minimum for Astro-2 led to a dramatic decrease in many airglow lines relative to the near-solar maximum conditions of Astro-1. Optically thick lines such as Ly$\alpha$ and O I $\lambda$1304 were reduced by a factor of 2–3 in

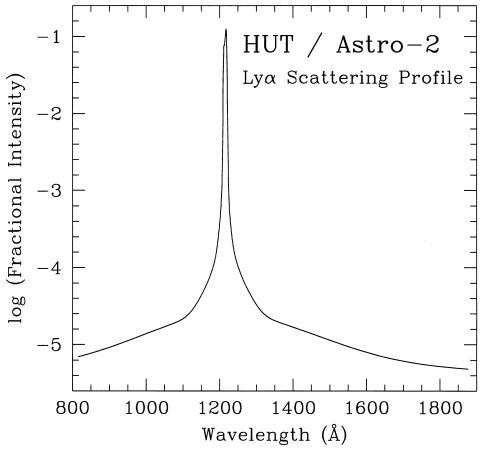


FIG. 6.—The profile of scattered Ly$\alpha$ is plotted as the flux per angstrom divided by the total line flux, derived from observations of four blank fields through the 20″ circular aperture with a total integration time of 7146 s.

intensity relative to Astro-1. Typical orbital night intensities for Ly$\alpha$ were about 1.5 kR (1 Rayleigh = $10^6$ photons cm$^{-2}$ s$^{-1}$ sr$^{-1}$), with variations depending on the particular line of sight. Optically thin lines such as O I $\lambda$1356 were down by nearly 1 order of magnitude relative to Astro-1.

Most airglow lines are weak enough that they affect only regions of the spectrum corresponding to the width of the aperture used for a particular observation. For the frequently used 20″ aperture this is about 15 Å. Line profiles derived from observations of blank fields suffice to characterize and remove these lines when rescaled to the observation of interest. Light from geocoronal Ly$\alpha$ scattered within the spectrograph is a more serious problem. While the holographically ruled grating has extremely low scattering properties, approximately $10^{-5}$ Å$^{-1}$ of the total intensity far from the line center, the strength of the Ly$\alpha$ airglow emission gives a scattered component to the background that is comparable to the detector dark count during orbital night. During orbital day and in the near wings of Ly$\alpha$, it dominates the background.

Observations of blank fields during orbital night were summed and fitted with a smoothly varying function to derive the Ly$\alpha$ scattering profile for each aperture used during the Astro-2 mission. Figure 6 shows the scattering profile obtained for 7146 s of integration on blank sky in four separate pointings through the 20″ aperture. Since the cores of Ly$\alpha$ and of O I $\lambda$1304 are affected by dead-time corrections and a continuously decreasing QDE, the best match for removing the scattered Ly$\alpha$ profile is obtained by scaling the model profile to the near wings in the 1159–1211 Å and 1221–1273 Å ranges.

## 4. SUMMARY

Silicon carbide coatings on the primary mirror and grating of HUT improved its performance relative to Astro-1 by more than a factor of 2 for the flight of Astro-2. We achieved a peak effective area of 24.1 cm$^2$ at 1160 Å with an inverse sensitivity of $7.09 \times 10^{-13}$ erg cm$^{-2}$ count$^{-1}$. Most of the first-order wavelength range of 820–1840 Å had an effective area exceeding the 10.4 cm$^2$ peak area of the Astro-1 instrument. Spectra of point sources showed a resolution of 2–4 Å. Dark counts were less than $10^{-3}$ counts s$^{-1}$ Å$^{-1}$ outside the SAA; grating-scattered geocoronal Ly$\alpha$ radiation made a comparable contribution to the background during orbital night and dominated the background rates during orbital day.

We derived our photometric calibration using multiple observations of the white dwarf HZ 43 and a white dwarf model atmosphere. Comparison of flux-calibrated observations of several other white dwarfs spanning a broad range in temperature to model atmosphere calculations shows our calibration to be accurate to about 5%. The instrument's sensitivity declined throughout the flight by as much as 27% at the short end of the wavelength range; most of this degradation occurred during the first third of the mission. A similar decrease in reflectivity seen in one of the witness mirrors in the telescope housing suggests either in-flight contamination or some oxidation of the silicon carbide coating.

The near-nominal performance of HUT throughout the 16 day mission plus the improved pointing stability relative to Astro-1 led to a total of 385 observations of 265 individual targets. A total on-target integration time of 205 hr over the 14 days of science operations gives an observing efficiency of better than 60%, a phenomenal performance for a low–Earth-orbit observatory.

We are grateful to our many colleagues and students on the HUT team at the Johns Hopkins University and the Applied Physics Laboratory, who have contributed greatly to the success of this project. We thank the payload processing team at Kennedy Space Center for their expert handling of the integration and preflight testing of the Astro-2 payload. We also thank Ritva Keski-Kuha and the staff of the Optical Thin Film Laboratory at Goddard Space Flight Center for their efforts in producing the successful SiC coatings of our grating and primary mirror. Finally, we thank the crew of STS-67 and the ground controllers at Johnson Space Center and Marshall Space Flight Center for all their efforts in making this mission a success. This work was supported by NASA contract NAS 5-27000 to the Johns Hopkins University.

## REFERENCES

Bergeron, P. 1993, in White Dwarfs: Advances in Observation and Theory, NATO ASI series, ed. M.A. Barstow (Dordrecht: Kluwer), 267
Bohlin, R. C., Colina, L., & Finley, D. S. 1995, AJ, in press
Davidsen, A. F. 1993, Science, 259, 327
Davidsen, A. F., et al. 1992, ApJ, 392, 264
Davidsen, A. F., Kriss, G. A., & Zheng, W. 1995, Nature, submitted
Espey, B. R., et al. 1995, ApJ, 454, L61
Finley, D. S., Koester, D., & Basri, G. 1995, in preparation
Grewing, M., et al. 1991, in Extreme-Ultraviolet Astronomy, ed. R. Malina & S. Bowyer (New York: Pergamon), 437
Herzig, H., Toft, A. R., & Fleetwood, C. M., Jr. 1993, Appl. Opt., 32, 1798
Holberg, J. B. 1991, in Extreme-Ultraviolet Astronomy, ed. R. Malina & S. Bowyer (New York: Pergamon), 8
Hummer, D. G., & Mihalas, D. 1988, ApJ, 331, 794
Hurwitz, M., & Bowyer, S. 1991, in Extreme-Ultraviolet Astronomy, ed. R. Malina & S. Bowyer (New York: Pergamon), 442
Keski-Kuha, R. A. M., Osantowski, J. F., Herzig, H., Gum, J. S., & Toft, A. R. 1988, Appl. Opt., 27, 2815
Keyes, C. D., et al. 1995, Faint Object Spectrograph Instrument Handbook, Version 6.0 (Baltimore: STScI)
Koester, D., Schulz, H., & Weidemann, V. 1979, A&A, 76, 262
Kriss, G. A. 1994, in ASP Conf. Proc. 61, Astronomical Data Analysis Software and Systems III, ed. D. R. Crabtree, R. J. Hanisch, & J. Barnes (San Francisco: ASP), 437
Kruk, J. W., et al. 1995, in preparation
McCandliss, S. R., et al. 1994, Proc. SPIE, 2011, 310
Rogerson, J. B., et al. 1973, ApJ, 181, L97